

# A Fresh Look at Diffuse Gamma-ray Emission from the Inner Galaxy

B. M. BAUGHMAN, W. B. ATWOOD, R. P. JOHNSON, T. A. PORTER, AND M. ZIEGLER Santa Cruz Institute for Particle Physics, University of California, Santa Cruz, CA 95064, U.S.A.

brian@scipp.ucsc.edu

**Abstract:** The Energetic Gamma-Ray Experiment Telescope (EGRET) experiment onboard the Compton Gamma-Ray Observatory (CGRO) has provided the most precise measurements of the  $\gamma$ -ray sky to date. The EGRET measurements of the diffuse emission across the sky show an excess above 1 GeV. This "GeV excess" has been a topic of great debate and interest since its original discovery by Hunter et al. in 1997. We have modified the GLAST simulation and reconstruction software to model the EGRET instrument. This detailed modeling has allowed us to explore the parameters of the EGRET instrument, in both its beam-test configuration and in-orbit on CGRO, in greater detail than has previously been published. We have found that the GeV excess is significantly increased when previously unaccounted for instrumental effects are considered. We will present a new measurement of diffuse  $\gamma$ -ray emission in the inner Galaxy.

### Introduction

The EGRET[1] telescope onboard the CGRO provided the most detailed look at the  $\gamma$ -ray sky to date. Before launch, the EGRET collaboration performed extensive testing [2] to characterize the instrument response to both charged particles and  $\gamma$ -rays. The instrument response functions found during these tests were the basis for constructing the EGRET exposure maps and thus the EGRET intensity sky maps. While there are references to a Monte Carlo simulation of the EGRET in a variety of EGRET publications [2, 3], it is clear from those publications that the simulations were preliminary in nature.

The simulation environment developed for use with the Gamma-ray Large Area Space Telescope (GLAST) [4] provides a basis on which we have developed our simulations. The simulation framework is based on GEANT4 [5, 6] which is well tested. We have constructed a geometric model of the EGRET instrument based on the most detailed information available. We have also included parametric response models for the EGRET sub-detectors. Both the geometric and response models are incorporated into the framework. Furthermore, we have integrated the Burst and Tran-

sient Source Experiment (BATSE) Mass Model of CGRO [7], used to estimate backgrounds in the BATSE instrument, with our model of the EGRET instrument.

Characterization of the EGRET instrument was extensive, consisting of a charged particle beam test and two  $\gamma$ -ray beam tests. However, it was not possible to test all configurations of the instrument, nor was it possible to examine the particle interactions outside of the detectors. The Monte Carlo framework we have constructed allows us to probe the instrument in detail and access information about the simulated events not available in the laboratory. Thus, we have been able to compare the differences between the EGRET in the beam test environments to the EGRET in its flight environment. Most notably, we have probed effects relating to the integration of the EGRET onto CGRO.

The EGRET was a pair-conversion telescope. As such, it required a method for rejecting charged particles entering the detector that might otherwise be treated as  $\gamma$ -rays. This was accomplished by the anti-coincidence system known as the Adome. The A-dome was a monolithic scintillator which was read out by 24 photo-multiplier tubes (PMTs) optically coupled to the lowest edge of the dome. During the EGRET beam test at the Stan-

ford Linear Accelerator Center (SLAC) it was discovered that the EGRET effective area ( $A_{eff}$ ) decreased at a rate that was faster than expected at high energies. The decrease was determined to be caused by "self-veto" [2], where an otherwise acceptable  $\gamma$ -ray event is vetoed by the A-dome when a secondary particle associated with the electromagnetic shower of the  $\gamma$ -ray in the instrument triggers a veto signal. The secondary particles can be either charged particle or X-rays which Compton scatter within the A-dome scintillator.

Our simulation environment has allowed us to explore the problem of self-veto with greater detail than was available during the calibration of the EGRET. Furthermore, we have simulated the instrument in the environment that the astrophysics data were taken, specifically within close proximity to the CGRO. Comparison between the beam test geometry and the flight geometry has produced some interesting results, primarily we find that the effect of self-veto is exacerbated by the EGRET being attached to the CGRO.

# **Analysis Methods**

The simulations have a variety of parameters which are related to the EGRET instrument response. Since we are primarily concerned with the effect of self-veto on the  $A_{eff}$  we limit our discussion to the relevant parameters. Effective vetoing of charged particle events passing through the Adome was dependent on the voltage settings of the readout PMTs. While in-flight, it was necessary to reduce the efficiency of vetoing charged particles during calibration of the calorimeter. Thus, the voltage settings on the readout PMTs were adjustable. To replicate this, we have implemented a threshold for energy measured at the PMTs for our simulated events. By measuring the  $A_{eff}$  for incident mono-energetic  $\gamma$ -rays at the same energies measured during the EGRET beam tests we are able to adjust this threshold for an optimized fit to the EGRET reported  $A_{eff}$  . We have also allowed for an overall normalization factor between the EGRET track finding algorithm and the one employed in our simulations.

The results of our optimization can be seen in Figs. 1 and 2. This optimization was performed using

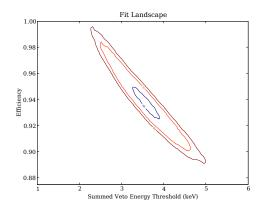


Figure 1: Optimization landscape with 68%, 95%, and 99% confidence contours. Summed veto threshold energy is calculated by summing the attenuated energy deposited within the A-dome.

simulated data in the beam geometry. Every attempt was made to mimic the EGRET triggering algorithm and spark chamber response. However, as was noted by the EGRET collaboration [2], below 300~MeV there are noticeable effects on the track finding due to the difference in efficiencies between tracking layers, thus we have performed our fit only for energies > 300~MeV.

For both the beam and flight geometries we generated 800000 events at near normal incidence in each of the 10 standard EGRET energy bins, plus three extended bins (10–20 GeV, 20–50 GeV, 50–120 GeV), using a spectrum proportional to  $E^{-2.1}$ ; this corresponds to the weighting used for generation of the EGRET exposure maps.

We construct scale factors for each of the 10 standard exposure energy ranges using the following formula:

$$F_{i} = \left(\frac{N_{i,flight}^{accepted}}{N_{i,flight}^{generated}}\right) / \left(\frac{N_{i,beam}^{accepted}}{N_{i,beam}^{generated}}\right)$$
(1)

where  $N_i$  is the number of events in energy bin i, the subscript labels refer to the geometrical configuration of the simulation (beam test or flight), and the superscript labels refer to the total number of generated events (generated) and the events accepted for reconstruction (accepted). These factors

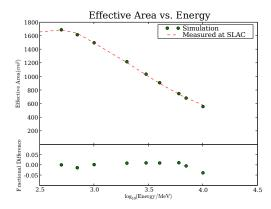


Figure 2: Simulated  $A_{eff}$  after optimizing the summed veto threshold energy to the beam test results from SLAC compared to the measured values.

are constructed assuming the same angular dependence as the published EGRET  $A_{eff}$  .

Extension of the EGRET effective area beyond 10 GeV has been done previously using the preliminary Monte Carlo mentioned earlier [8]. Our extension uses a similar approach. The exposure map for the 4–10 GeV bin is used as a basis for all higher energy bins. The exposure maps for the energy bins 10–20 GeV, 20–50 GeV, and 50–120 GeV, are generated using a scaling factor for each higher energy bin that accounts for the relative difference between the number of events generated and accepted for reconstruction in that bin compared with the number of events for the 4–10 GeV bin. The following formula is used to create the scaling factors:

$$F_{HE,j} = \left(\frac{N_{j,flight}^{accepted}}{N_{j,flight}^{generated}}\right)/A_9$$
 (2)

$$A_9 = \left(\frac{N_{9,beam}^{accepted}}{N_{9,beam}^{generated}}\right) \tag{3}$$

where j=10–20, 20–50, 50–100 GeV, the superscripts and subscripts have the same meaning as in Eq. 1, and  $N_{9,beam}^{accepted}$  and  $N_{9,beam}^{generated}$  are the number of accepted and generated events in the beam configuration for the 4–10 GeV bin, respectively.

Constructing the scaling factors as described reduces the possibility of systematic effects unrelated to changes in geometry. The ratio of flight geometry performance to beam test geometry performance should be invariant to effects unrelated to the change in geometry. The performance for each geometry has been examined in detail and there are no unanticipated effects that might introduce large systematic errors to our results.

#### Results

The scale factors calculated above are applied to the corresponding EGRET exposure maps. All the scaling factors found imply a systematically lower  $A_{eff}$  at high energies. This implies that each  $\gamma$ -ray measured is more significant than previously thought, leading to a systematic increase in both the integrated flux as well as the hardness of the spectra measured by the EGRET.

We have re-analyzed the EGRET data set in the inner Galaxy,  $0.5^{\circ} < |l| < 30^{\circ}$  and  $0.5^{\circ} < |b| < 6^{\circ}$ , using our re-scaled exposure maps. For comparison we have also analyzed two commonly accepted GALPROP [9] models, 599278 [10] and 6002029RE [11]. The GALPROP model 599278 is constructed by assuming the observed radiation, gas, and cosmic-ray distributions are representative of the Galaxy at large. This is referred to as the "conventional" model. 6002029RE has been modified to better reproduce the EGRET observations, specifically "secondary antiproton data were used to fix the Galactic average proton spectrum, while the electron spectrum is adjusted using the spectrum of diffuse emission itself"[10]. This is known as the "optimized" model. These models were run in their published configurations, except we changed the energy and skymap binning to correspond to the EGRET skymaps. In the following, we denote the runs for these models as 599278EG and 6002029EG, respectively. Fig. 3 shows the  $E_{\gamma}^2 dN_{\gamma}/dE_{\gamma}$  for our 599278EG and 6002029EG GALPROP models as well as the re-scaled and original EGRET measurements.

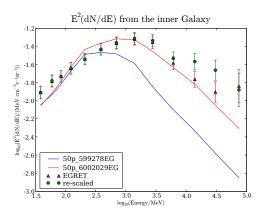


Figure 3: Comparison of  $E_{\gamma}^2 dN_{\gamma}/dE_{\gamma}$  spectra for  $0.5^{\circ} < |l| < 30^{\circ}$  and  $0.5^{\circ} < |b| < 6^{\circ}$ .

## **Conclusions**

The re-scaled EGRET spectrum for the inner Galaxy shows an increased excess when compared to previous results. When compared with the conventional model, the EGRET excess has a reduced  $\chi^2$  of 18.8 and 24.7 for the original and re-scaled EGRET measurements, respectively. For the optimized model, the EGRET excess has a reduced  $\chi^2$  of 1.9 and 3.4 for the original and re-scaled EGRET measurements, respectively. This analysis indicates that the GeV excess may be larger than previously thought. It is important to note that while the GeV excess is dramatic with respect to the conventional GALPROP model (599278EG) it is much reduced with respect to the optimized model (6002029EG).

### Acknowledgments

We would like to thank the thoughtful criticism and suggestions of Gottfried Kanbach (MPE), Seth Digel (SLAC), Olaf Reimer (Stanford), Andy Strong (MPE), Donald Kniffen (GSFC), and Dave Thompson (GSFC), all of whose input proved invaluable.

This work is partially supported by the United States Department of Energy through grant DE-FG02-04ER41286. Further support was provided by NASA grant PY-1775.

## References

- [1] G. Kanbach *et al.*, Space Science Reviews **49**, 69 (1988).
- [2] D. J. Thompson et al., ApJS 86, 629 (1993).
- [3] P. Sreekumar *et al.*, ApJ **494**, 523 (1998), astro-ph/9709257.
- [4] W. B. Atwood, Nuclear Instruments and Methods in Physics Research A 342, 302 (1994).
- [5] GEANT4, S. Agostinelli *et al.*, Nucl. Instrum. Meth. **A506**, 250 (2003).
- [6] J. Allison *et al.*, IEEE Trans. Nucl. Sci. **53**, 270 (2006).
- [7] S. E. Shaw *et al.*, A&A **398**, 391 (2003), arXiv:astro-ph/0211424.
- [8] D. J. Thompson, D. L. Bertsch, and R. H. O'Neal, Jr., ApJS 157, 324 (2005), 2004astro.ph.12376T.
- [9] A. W. Strong and I. V. Moskalenko, ApJ 509, 212 (1998), arXiv:astro-ph/9807150.
- [10] A. W. Strong, I. V. Moskalenko, and O. Reimer, ApJ 613, 962 (2004), arXiv:astroph/0406254.
- [11] A. A. Abdo *et al.*, ApJ **658**, L33 (2007), arXiv:astro-ph/0611691.